ASTM INTERNATIONAL

Materials Performance and Characterization

M. Doddamani,[1] G. Parande,[2] V. Manakari,[2] I. G. Siddhalingeshwar,[2] V. N. Gaitonde,[2] and N. Gupta[3]

DOI: 10.1520/MPC20160113

Wear Response of Walnut-Shell-Reinforced Epoxy Composites

VOL. 6 / NO. 1 / 2017

Materials Performance and Characterization

doi:10.1520/MPC20160113 / Vol. 6 / No. 1 / 2017 / available online at www.astm.org

M. Doddamani,[1] G. Parande,[2] V. Manakari,[2] I. G. Siddhalingeshwar,[2] V. N. Gaitonde,[2] and N. Gupta[3]

Wear Response of Walnut-Shell-Reinforced Epoxy Composites

Reference

Doddamani, M., Parande, G., Manakari, V., Siddhalingeshwar, I. G., Gaitonde, V. N., and Gupta, N., "Wear Response of Walnut-Shell-Reinforced Epoxy Composites," *Materials Performance and Characterization*, Vol. 6, No. 1, 2017, pp. 55–79, http://dx.doi.org/10.1520/MPC20160113. ISSN 2165-3992

ABSTRACT

Present work utilizes agricultural by-product, walnut shell, as reinforcing filler in epoxy matrix for investigating dry sliding wear behavior using a pin-on disc wear-testing machine. Effects of sliding velocity (0.5–1.5 m/s), normal load (10–50 N), sliding distance (1000–3000 m) and filler content (10–30 wt. %) on wear rate (W_t), specific wear rate (W_s) and coefficient of friction (μ) are investigated. The experiments were planned as per design of the experiments scheme and the wear characteristics were analyzed through response surface modeling (RSM) method. The lowest W_t of 1.1 mm^3/km was noted for 1.5 m/s sliding velocity with 30-wt. % filler content. Sliding distance did not have a significant influence on W_s above a critical load of 40 N. The minimum μ was observed at 1-m/s sliding velocity, 40-N load, 1000-m sliding distance, and 30-wt. % filler. Lower values of W_t and μ at higher walnut-shell loadings support feasibility of using such composites in wear-prone applications. The wear mechanism was determined in the composites using extensive scanning electron microscopic observations.

Keywords

walnut shell, wear, design of experiments, friction, response surface methodology

Manuscript received September 30, 2016; accepted for publication January 10, 2017; published online February 22, 2017.

[1] Advanced Manufacturing Laboratory, Dept. of Mechanical Engineering, National Inst. of Technology Karnataka, Surathkal, India

[2] BVB College of Engineering and Technology, Hubli, Karnataka, India, e-mails: gururaj.parande@gmail.com; mbvyasaraj@gmail.com

[3] Composite Materials and Mechanics Laboratory, Mechanical and Aerospace Engineering Dept., Tandon School of Engineering, New York Univ., Brooklyn, NY 11201 (Corresponding author), e-mail: ngupta@nyu.edu

Introduction

A variety of filler micro- and nano-scale materials that can result in low-cost composites with high mechanical properties and performance are being explored [1–3]. Use of agricultural by-products as fillers can help in developing low-cost polymer matrix composites (PMCs) [4]. Natural filler reinforced PMCs have been developed with attractive properties, such as high specific strengths and modulus, impact strength, and ballistic performance [5,6]. Increased use of lignocelluloses as reinforcing fillers is reported in applications in automotive, siding, and decking industries [7]. Walnut shell is one such naturally available agricultural by-product that can be utilized in engineering applications.

The main characteristic of walnut-shell microstructure is the highly lignified stone cells [8]. This structure is accredited to the relatively short and isodiametric cells of nutshells known as sclereids whose secondary walls are lignified and vary in thickness. Cell walls accounting to 90 % of total volume result in higher strength and stiffness [9]. Walnut-reinforced PMCs may have competitive advantage over wood in outdoor applications requiring a high dimensional stability, such as deck flooring or siding, because of lower hygroscopic content (cellulose and hemicellulose) and higher hydrophobic content (lignin and extractives) [10,11]. Many of these applications require high wear resistance for long product life. Such applications have also motived studies on tribological properties of PMCs [12,13]. Incorporation of organic and inorganic fillers, as well as fly ash cenospheres [14,15], glass [16], carbon [17], and aramid fibers, has evolved to improve the wear performance of polymers. The wear resistance of polymers was found to improve with the addition of nano SiC, CuO, TiO_2, ZnO, and ZrO_2 [18], even at low filler contents [19].

Walnut-shell powder has been used as a reinforcement in PMCs and their physical and mechanical properties have been investigated [20]. It was noted that the properties of PMCs can be enhanced with the help of a coupling agent between walnut particles and the polymer matrix [21]. Walnut-reinforced (10–40 wt. %) epoxy matrix composites showed increased compressive strength with increasing walnut particle content, but the moisture uptake also increased [22]. Addition of walnut-shell powder to polypropylene resulted in increased tensile, flexural, and moisture-absorption characteristics with a decline in impact strength [23]. Qi et al. [24] addressed utilization of 0–14.6 vol. % alkaline-treated walnut-shell powders as a functional filler in five non-asbestos materials containing jute fibers from biomass, including several from natural resources, such as wollastonite, basalt fibers, zircon, barite, and vermiculite. The coefficient of friction (COF) and wear rate of these hybrid samples found to be effectively improved. Surface modifications of fillers and hybridization effect of multiple fillers might increase the processing complexity increasing cost factor. Thereby, it would be worthwhile to discuss the wear investigations of walnut-reinforced epoxy composites at higher filler loadings.

The present work studies the walnut-shell-reinforced epoxy matrix composites for wear-resistant applications. A pin-on-disc tribometer is used to conduct the experiments using full factorial design (FFD). Sliding velocity, normal load, sliding distance, and filler content are the study variables. Further, based on experimental values of response surface modeling (RSM), mathematical expressions are proposed for wear rate (W_t), specific wear rate (W_s), and coefficient of friction (μ). For

interpolation between the scarce experimental data, these expressions are used to capture the overall trend. Analysis of variance (ANOVA) is used to find the most influential parameter on the response. Use of such statistical tools allows the study of interactions among the process parameters.

Materials and Methods

MATERIALS

The matrix used in the present investigation comprises a diglycidyl ether of bisphenol A (DGEBA) epoxy resin (LAPOX L-12) and a room temperature curing polyamine hardener (K-6) containing a tetra-amine functional group supplied by Yuje Marketing (Bangalore, Karnataka, India). The filler material used in this study was as-received walnut shell supplied by Super Minerals Corporation (Mumbai, Maharashtra, India). The densities of walnut-shell powder and cured neat epoxy resin were found to be 1522.5 and 1192.6 kg/m^3, respectively. Walnut shell contains cellulose (60 %), lignin (30 %), methoxyl (6.5 %), ash (1.5 %), cutin (1 %), fatty acids (0.2 %), nitrogen (0.1 %), and chlorine (0.1 %) [23,25].

SAMPLE PREPARATION

The composite fabrication procedure consists of mixing walnut-shell particles in desired weight fraction (10, 20, and 30 wt. %) with the resin and hardener. The processing is carried out at room temperature. The mixture is gently stirred to obtain homogeneous slurry, which is degassed for 10 min and then cast in aluminum molds of dimensions $100 \times 100 \times 16$ mm^3. The cast slabs are cured at room temperature for 24 h and post cured at 100°C for 3 h. Neat resin specimens are also fabricated for comparison. The mold was coated with a silicone release agent for easy removal of cast slabs. Wear-test specimens of dimension $12 \times 12 \times 25$ mm^3 were cut from the cast slabs using a diamond saw.

EXPERIMENTAL PROCEDURE

Process parameters identified in the present work are sliding velocity (v), normal load (F), sliding distance (d), and filler weight fraction (R) affecting the responses W_t, W_s, and μ. Pilot experiments were conducted to freeze the range of the process parameters. Three levels for each of the four parameters were selected to study the influence of parameters on friction and sliding wear behavior through FFD of experiments. Accordingly, 81 trials based on FFD were planned [26,27] with five replicates each. Process parameters and their levels are presented in **Table 1**. The

TABLE 1

Process parameters and their levels.

	Level		
Parameter	1	2	3
Sliding velocity (v), m/s	0.5	1	1.5
Applied normal load (F), N	10	30	50
Sliding distance (d), m	1000	2000	3000
Filler content (R), wt. %	10	20	30

TABLE 2

Density and void content of the neat resin and walnut-shell-reinforced epoxy composites.

R (wt. %)	ρ_{ct} (g/cm^3)	ρ_{ce} (g/cm^3)	V_v (vol. %)
0	1.19	1.19 ± 0.01	0.37
10	1.23	1.20 ± 0.03	1.68
20	1.26	1.22 ± 0.04	2.03
30	1.29	1.25 ± 0.06	2.35

12×12 mm^2 face of the specimens was loaded against the disc with the loads of 10, 30, and 50 N corresponding to initial contact pressures of 0.07, 0.21, and 0.35 MPa, respectively. The sliding velocity is limited to 1.5 m/s to avoid issues related to strain-rate sensitivity of the resin [28].

DENSITY MEASUREMENT

Experimental density (ρ_{ce}) is evaluated using Archimedes principle by weighing the specimens first in air and then in water. The theoretical density (ρ_{ct}) is calculated using rule of mixtures as,

$$\rho_{ct} = \frac{1}{\frac{M_f}{\rho_f} + \frac{M_m}{\rho_m}} \tag{1}$$

where:

M and ρ = the weight fraction and density, respectively,
the suffixes f and m = filler and matrix, respectively, and
the density of the epoxy matrix = 1192.6 kg/m^3.

The volume fraction of matrix porosity (V_v) in the composite is determined by,

$$V_v = \frac{\rho_{ct} - \rho_{ce}}{\rho_{ct}} \tag{2}$$

Theoretical and experimental densities of the composites and matrix porosities are presented in **Table 2**. The matrix porosity is observed to increase with increasing filler content in the specimen. However, in all cases the matrix porosity content is below 2.35 %.

DRY SLIDING WEAR TEST

Wear tests in dry sliding mode were carried out at ambient temperature using a pin-on-disc wear tester (DUCOM, India) as per ASTM G99-05 (2016) standard [29]. A disc made of hardened chromium steel (EN-31, hardness 62 HRC) was used as the counter body against the pin. The tests were conducted at 240 rpm on tracks of different diameters (40, 80, and 120 mm). With the proposed design of experiments test duration, load, and sliding speed were varied. Normal force was applied through a lever mechanism. The dead weight (load), which is mounted on the pan of the lever mechanism, ensures constant normal force during the test.

Both pin and disc were polished against 600-grit SiC paper before the test for keeping the initial surface roughness parameter (R_a = 0.11 μm) constant for all the tests. Further, it ensures proper contact between the sample and the counter face.

Height loss and frictional force were recorded by a computer-aided data-acquisition system. Using the pin cross-section area, height loss is converted to volume loss. The wear rate is defined as the volume loss per unit sliding distance. From sliding speed and time elapsed, sliding distance is computed. W_t is estimated by

$$W_t = \frac{V_C - V_B}{d_C - d_B} \tag{3}$$

where:

V = the wear volume,

d = the sliding distance, and

subscripts B and C = beginning and end of steady-state wear, respectively.

The wear rate varies with the applied normal load and is independent of sliding distance. Reciprocal of wear rate is wear resistance, which is given by

$$W_R = W_t^{-1} \tag{4}$$

W_s accounts for the load bearing ability of the material and is represented by

$$W_s = \frac{W_t}{F} \tag{5}$$

where:

F = the normal load applied during wear test.

μ is defined as

$$\mu = \frac{F_T}{F_N} \tag{6}$$

where:

F_T = the tangential force required to produce sliding and is obtained from the steady-state wear regime, and

F_N = the normal force between the mating surfaces.

SCANNING ELECTRON MICROSCOPY

The walnut-shell powder, as-fabricated specimens, and wear surfaces are investigated using a field emission scanning electron micrograph (Hitachi S-4300, Tokyo, Japan). The microscope is equipped with secondary electron and back-scattered electron detectors. The specimens were sputter coated with a conducting layer of gold before imaging (JEOL JFC-1200 Fine Coater, Tokyo, Japan).

Results and Discussion

Fig. 1a and **1b** presents micrographs of walnut-shell powder in as-received condition. Composite with 30-wt. % loading is presented in **Fig. 1c**. Walnut-shell powder is highly irregular in shape with 40–50 μm size (**Fig. 1a**). Higher magnification (**Fig. 1b**) reveals porous flaky structure, which acts as an effective interlock with the epoxy resin. **Fig. 2a** present experimental setup of wear test. A representative set of results obtained from the wear testing is presented in **Fig. 2b** and **2c**. Height loss (**Fig. 2b**) and frictional force (**Fig. 2c**) are plotted with respect to the time. These representative results are obtained on a specimen reinforced with 30 wt. % filler under the

FIG. 1 Micrographs of walnut-shell powder at (a) lower magnification, (b) higher magnification, and (c) epoxy resin reinforced with 30-wt. % filler.

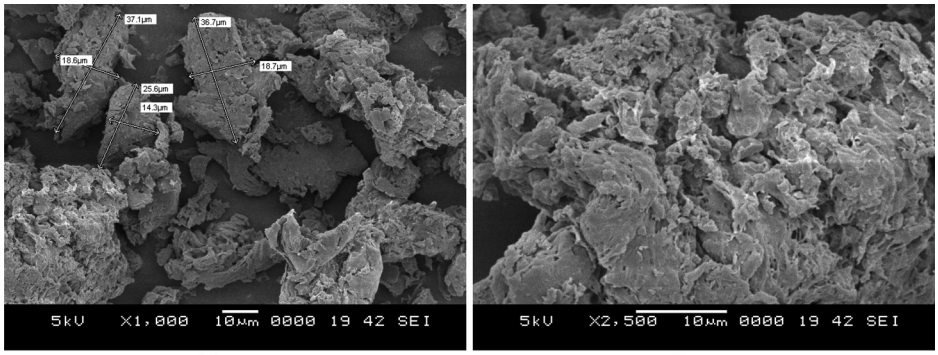

(a) (b)

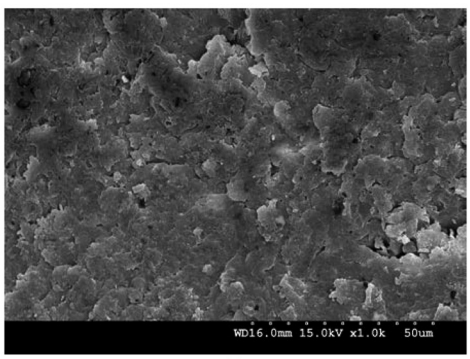

(c)

conditions of $F = 50$ N, $d = 3000$ m, and $v = 1.5$ m/s. An initial transition period is observed after which the wear achieves a steady state as observed in **Fig. 2b**. A similar behavior is demonstrated by composites as well, although the transient region is less pronounced. Further, height loss in neat resin specimens is twice that in composite specimens at 2000 s time as observed in **Fig. 2b**. This observation implies that the walnut shell is effective in reducing the wear of composites. Further, frictional force shows decreasing trend in composite with increasing time after reaching the peak value, whereas a plateau is observed in case of neat resin specimens. Frictional force in composite specimens drops by 14 % compared to neat resin for the same time interval, which highlights the effectiveness of walnut shell in these composites for wear applications.

EFFECTS OF INDIVIDUAL PARAMETERS

Tables 3–5 present the experimental results of W_t, W_s, and μ for sliding velocities of 0.5, 1, and 1.5 m/s, respectively. The values reported in these tables are averages of four replicates. ANOVA results based on these tables are presented in **Table 6**. The developed RSM models were also tested through coefficient of determination (CoD) (**Table 6**), which is the proportion of variation in the parameter explained by the model. CoD value is found to be high in case of W_t and W_s, indicating a good

FIG. 2 (a) Experimental wear-test setup. A representative set of graphs obtained from the wear test: (b) height loss, and (c) frictional force for $F = 50$ N, $d = 3000$ m, and $v = 1.5$ m/s.

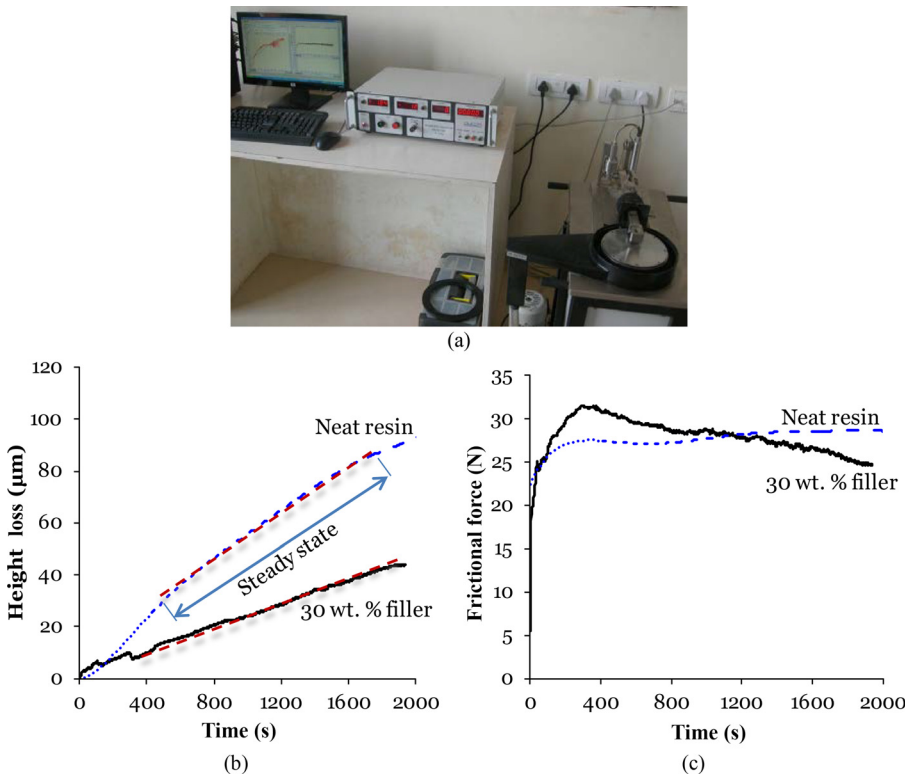

correlation between the predicted and the experimental values, which is desirable. The μ is found to fluctuate with time, which is common for the dry sliding wear of composites. This fluctuation in μ is attributed to the formation of a lubricating film, mainly of the matrix material during dry sliding wear of composites [30]. To accommodate these fluctuations with respect to time, 95 % confidence interval for μ is chosen in **Table 6** instead of 99 % set for the other parameters.

ANALYTICAL MODELS

Based on the independent parameters (v, F, d, and R), RSM based expressions are proposed for the dependent variables (W_t, W_s, and μ). The quadratic equation considering two-factor interactions is given in previous studies [26,27] as,

$$Y = b_0 + b_1 v + b_2 F + b_3 d + b_4 R + b_{11} v^2 + b_{22} F^2 + b_{33} d^2 + b_{44} R^2 + b_{12} vF + b_{13} vd + b_{14} vR + b_{23} Fd + b_{24} FR + b_{34} dR \quad (7)$$

where:

Y = the desired characteristic, and

$b_o, b_1, \ldots b_{34}$ = the regression coefficients to be determined.

The regression coefficients of the quadratic model are estimated by [26,31]:

$$b = (X^T X)^{-1} X^T Y \quad (8)$$

TABLE 3

Experimentally measured W_t, W_s, and μ for different F, d, and R, at $v = 0.5$ m/s.

Process Parameter Settings			Outcome		
F (N)	d (m)	R (wt. %)	W_t (mm^3/km)	W_s (mm^3/N-km)	μ
10	1000	10	4.40	0.4400	0.431
		20	3.98	0.3980	0.575
		30	2.82	0.2824	0.483
	2000	10	3.27	0.3270	0.622
		20	2.42	0.2420	0.705
		30	2.18	0.2180	0.890
	3000	10	2.80	0.2800	0.579
		20	1.95	0.1948	0.666
		30	1.78	0.1782	0.468
30	1000	10	4.98	0.1660	0.456
		20	4.36	0.1453	0.494
		30	3.02	0.1008	0.553
	2000	10	3.76	0.1253	0.562
		20	2.73	0.0910	0.597
		30	2.47	0.0824	0.333
	3000	10	3.06	0.1020	0.454
		20	2.32	0.0773	0.605
		30	2.25	0.0750	0.283
50	1000	10	7.23	0.1446	0.575
		20	6.24	0.1248	0.496
		30	3.95	0.0790	0.410
	2000	10	4.21	0.0842	0.542
		20	3.68	0.0736	0.661
		30	3.24	0.0648	0.367
	3000	10	3.40	0.0680	0.527
		20	3.44	0.0688	0.596
		30	3.43	0.0686	0.602

where:

b = the matrix of parameter estimates,

X = the calculation matrix that includes linear, quadratic, and interaction terms, and

X^T = the transpose of X.

The quadratic expressions as determined by multiple regression analysis of the experimental results to predict W_t, W_s, and μ are given by,

$$W_t = 6.65 - (1.92 \times \mathrm{v}) + (1.6 \times 10^{-2} \times F) - (9.3 \times 10^{-4} \times d) - (8.57 \times 10^{-2} \times R) + (4.25 \times 10^{-1} \times \mathrm{v}^2) + (6.65 \times 10^{-4} \times F^2) - (9.3 \times 10^{-8} \times d^2) + (7.19 \times 10^{-5} \times R^2) - (2.69 \times 10^{-3} \times \mathrm{v} \times F) + (3.08 \times 10^{-4} \times \mathrm{v} \times d) - (0.001.08 \times 10^{-3} \times \mathrm{v} \times R) - (5.4 \times 10^{-6} \times F \times d) - (4.8 \times 10^{-4} \times F \times R) + (1.85 \times 10^{-5} \times d \times R) \quad (9)$$

TABLE 4

Experimentally measured W_t, W_s, and μ for different F, d, and R, at $v = 1$ m/s.

Process Parameter Settings			Outcome		
F (N)	d (m)	R (wt.%)	W_t (mm^3/km)	W_s (mm^3/N-km)	μ
10	1000	10	3.84	0.3840	0.815
		20	3.41	0.3410	0.594
		30	2.43	0.2430	0.305
	2000	10	3.29	0.3290	0.601
		20	2.83	0.2834	0.570
		30	2.51	0.2510	0.574
	3000	10	1.87	0.1870	0.670
		20	1.29	0.1297	0.436
		30	1.82	0.1816	0.600
30	1000	10	4.29	0.1430	0.309
		20	3.73	0.1243	0.400
		30	2.71	0.0903	0.255
	2000	10	3.34	0.1113	0.634
		20	3.06	0.1020	0.611
		30	2.92	0.0973	0.552
	3000	10	3.19	0.1063	0.612
		20	1.52	0.0507	0.398
		30	1.70	0.0567	0.671
50	1000	10	4.82	0.0964	0.443
		20	4.89	0.0978	0.530
		30	3.67	0.0734	0.526
	2000	10	5.27	0.1054	0.157
		20	3.76	0.0752	0.483
		30	3.41	0.0682	0.534
	3000	10	2.90	0.0580	0.394
		20	1.91	0.0382	0.439
		30	2.67	0.0534	0.472

$$W_s = 0.78 - (0.1 \times \mathrm{v}) - (2.04 \times 10^{-2} \times F) - (8.8 \times 10^{-5} \times d) - (8.66 \times 10^{-3} \times R) + (7.79 \times 10^{-3} \times \mathrm{v}^2) + (1.72 \times 10^{-4} \times F^2) - (4.9 \times 10^{-9} \times d^2) + (2.63 \times 10^{-5} \times R^2) + (1.03 \times 10^{-3} \times \mathrm{v} \times F) + (1.11 \times 10^{-5} \times \mathrm{v} \times d) + (2.1 \times 10^{-4} \times \mathrm{v} \times R) + (0.000001.36 \times 10^{-6} \times F \times d) + (9.18 \times 10^{-5} \times F \times R) + (8.92 \times 10^{-7} \times d \times R) \quad (10)$$

$$\mu = 0.57 - (2.91 \times 10^{-1} \times \mathrm{v}) - (8.39 \times 10^{-3} \times F) + (1.93 \times 10^{-4} \times d) + (8.72 \times 10^{-3} \times R) + (3.77 \times 10^{-2} \times \mathrm{v}^2) + (5.68 \times 10^{-5} \times F^2) - (5.3 \times 10^{-8} \times d^2) - (4 \times 10^{-4} \times R^2) + (1.84 \times 10^{-3} \times \mathrm{v} \times F) + (4.86 \times 10^{-5} \times \mathrm{v} \times d) + (6.39 \times 10^{-4} \times \mathrm{v} \times R) - (3.5 \times 10^{-7} \times F \times d) + (1.08 \times 10^{-4} \times F \times R) + (1.06 \times 10^{-6} \times d \times R) \quad (11)$$

TABLE 5

Experimentally measured W_t, W_s, and μ for different F, d, and R, at $v = 1.5$ m/s.

Process Parameter Settings			Outcome		
F (N)	d (m)	R (wt.%)	W_t (mm^3/km)	W_s (mm^3/N-km)	μ
10	1000	10	3.43	0.3430	0.338
		20	2.92	0.2920	0.340
		30	2.26	0.2260	0.461
	2000	10	3.14	0.3140	0.407
		20	2.21	0.2214	0.636
		30	1.98	0.1980	0.380
	3000	10	1.97	0.1970	0.591
		20	1.72	0.1720	0.680
		30	1.10	0.1100	0.448
30	1000	10	3.79	0.1263	0.551
		20	3.15	0.1050	0.522
		30	2.63	0.0876	0.306
	2000	10	3.48	0.1160	0.489
		20	2.92	0.0973	0.546
		30	2.41	0.0803	0.667
	3000	10	2.80	0.0933	0.564
		20	2.39	0.0797	0.550
		30	1.20	0.0400	0.372
50	1000	10	4.73	0.0946	0.488
		20	4.38	0.0876	0.286
		30	3.31	0.0662	0.330
	2000	10	4.51	0.0902	0.450
		20	4.83	0.0966	0.537
		30	2.81	0.0562	0.610
	3000	10	3.81	0.0762	0.508
		20	2.79	0.0558	0.522
		30	1.81	0.0362	0.568

TABLE 6

Summary of ANOVA results and coefficient of determination (CoD) values for the regression model.

	Sum of Squares		Degrees of Freedom		Mean Square			
Parameter	Regression	Residual	Regression	Residual	Regression	Residual	CoD	F-Ratio
W_t	85.587	13.377	14	66	6.113	0.2027	0.865	30.16[a]
W_s	0.7038	0.0328	14	66	0.0502	0.0005	0.955	101.02[a]
μ	0.3282	0.9738	14	66	0.0234	0.0147	0.252	1.59[b]

[a] F-table = 2.36. Significance at 99 % confidence interval.
[b] F-table = 1.46. Significance at 95 % confidence interval.

where:

v = represented in m/s, F in N, d in m, R in (wt. %), W_t in mm^3/km, and W_s in mm^3/N-km.

The adequacy of these constructed models/expressions is confirmed through analysis of variance (ANOVA) [26,31]. As per ANOVA, the computed value of F-ratio of developed model/expression should be more than the corresponding value in F-table (**Table 6**) for the model to be adequate for a specified confidence interval. F-ratio is mathematically expressed as the ratio of mean square of regression model to the mean square of residual error.

The RSM based models 9–11 are used to predict W_t, W_s, and μ by substituting appropriate values of v, F, d, and R to identify the parameter that has the most dominant influence. Results of the parametric study are presented in **Figs. 3–5** by considering two parameters at a time. These plots can be helpful in understanding the general trends between various parameters. It can be observed from **Fig. 3a** that W_t increases with increasing F but decreases with increasing v. Similarly, **Fig. 3b** shows that the W_t tends to decrease with increasing both R and v. **Fig. 4** shows that the W_s decreases with v, F, R, and d. μ decreases with increasing F and v (**Fig. 5a**). **Fig. 5b** shows that μ increases with increasing R and d up to 20 wt. % of the filler content. Surface roughness, which is not a parameter for the present work, may also influence the wear behavior of materials.

Residual analysis is used to check the accuracy of the proposed models (Eqs 9–11). For regression analysis to be valid, it is essential that residuals should be normally distributed. Normal probability plots of the residuals for W_t, W_s, and μ are presented in **Fig. 6**. As seen from these plots, residual errors are normally distributed except for a few points. The proposed models adequately support least square fit of measured and predicted values for W_t, W_s, and μ (**Fig. 7**). The developed models can be used to predict the intermediate wear parameters of walnut-shell/epoxy composites.

FIG. 3 The trend of W_t with respect to individual parameters estimated by the model: (a) F and v and (b) d and R.

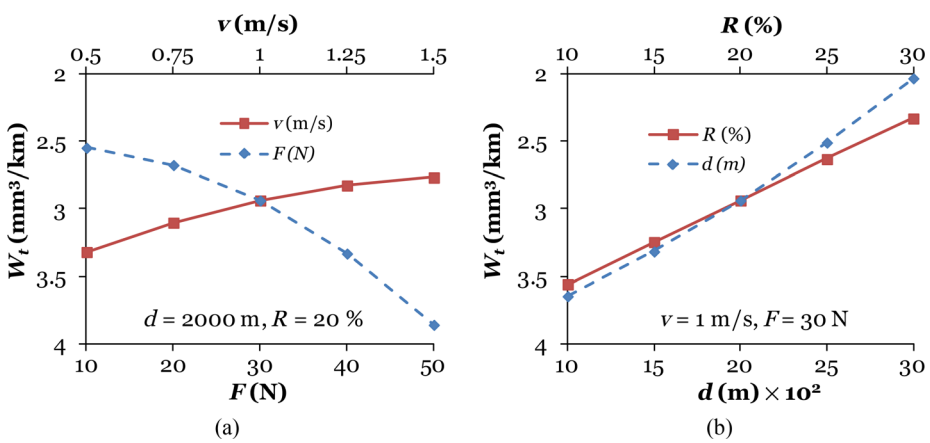

FIG. 4 The trend of W_s plotted with respect to individual parameters estimated by the model: (a) F and v and (b) d and R.

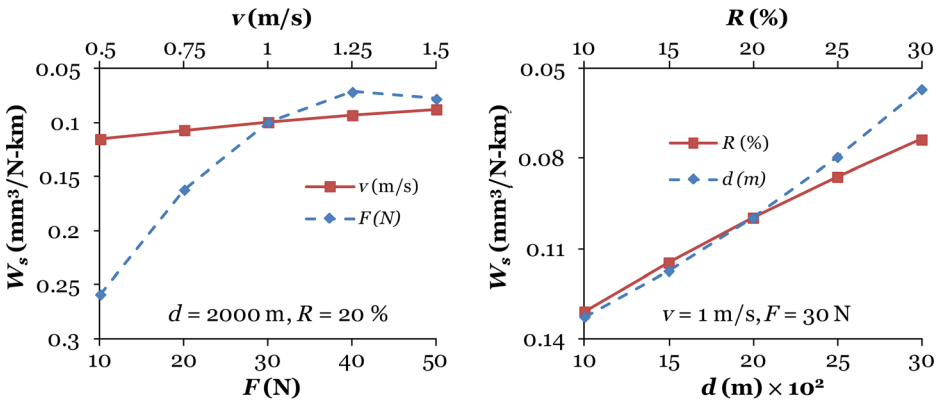

EFFECTS OF TWO-PARAMETER INTERACTIONS

Equations 9–11 are used to develop the interaction plots as presented in **Figs. 8–10** based on the matrix of **Table 7**. These graphs were drawn considering two parameters at a time, whereas the other two parameters were kept at the middle value.

Wear Rate

Interaction effect of process parameters on W_t are presented in **Fig. 8**. W_t is observed to decrease monotonically for any specified value of F, d, and R (**Fig. 8a–8c**). **Fig. 8a** shows that W_t increases with F. W_t decreases with increase in d (**Fig. 8b**) and R (**Fig. 8c**). These graphs can be useful in selecting a combination of parameters that can provide desired wear characteristics.

At higher loads, higher frictional thrust could result in increased debonding of particles from the epoxy resin leading to higher wear rate [32,33]. Similar effect of normal load on volumetric wear rate during the wear testing of epoxy composites

FIG. 5 The trend of μ plotted with respect to individual parameters estimated by the model: (a) F and v and (b) d and R.

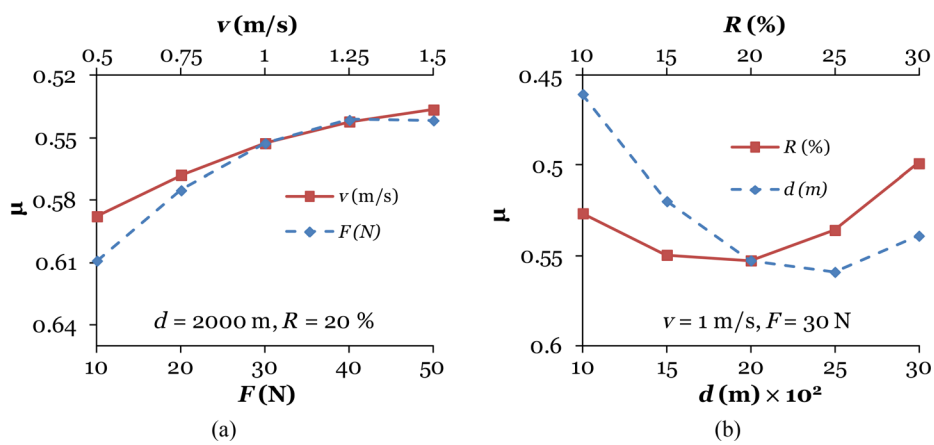

FIG. 6 Normal probability plot of residuals for (a) W_t, (b) W_s, and (c) μ.

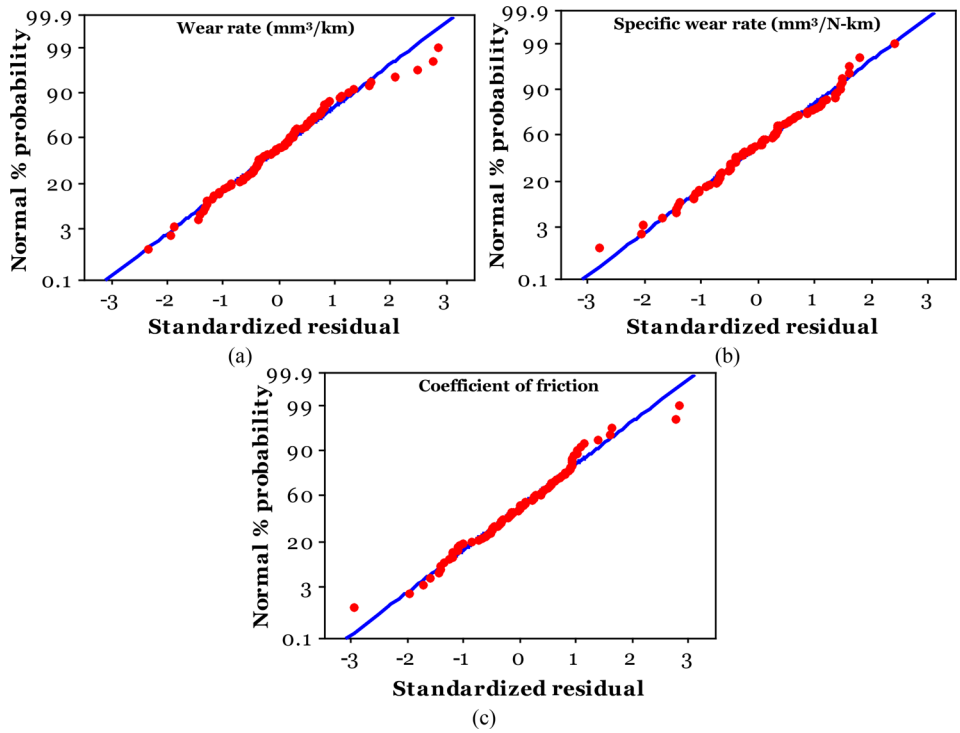

was observed by Kanchanomai et al. [34]. The estimated W_t as a function of v and d is presented in **Fig. 8b**. For increasing v from 0.5 to 1.5 m/s and d of 1000–3000 m, W_t decrease by 19.8 % and 38.2 %, respectively. High initial wear rate at lower sliding velocities is because of the fracture of irregular asperities of walnut-shell particles. However, with increasing sliding velocity, wear progresses with smoothening of asperities of both epoxy and irregular walnut-shell particles leading to enhanced wear resistance. Rao and Das [35] found that surface quality and surface chemistry vary with increased sliding distance resulting in divergence in wear rate with sliding distance.

Fig. 8c shows that the W_t decreases with the increasing v and R. Formation of transfer film on the counter face at higher sliding velocities is likely the reason for such an observation [18,32,36]. W_t decreases with increase in R, drop being more prominent at higher filler content (30 wt. %) owing to presence of higher volume of hard walnut-shell particles. Chauhan and Thakur [33] also reported that higher filler loading could reduce the wear rate to a large extent. In the present investigation, the minimum wear rate of 1.1 mm^3/km was obtained for a combination of higher sliding velocity (1.5 m/s) with 30 wt. % filler content.

The W_t as a function of R at different F is presented in **Fig. 8d**. W_t decreases drastically with increased R and F. It is known that, the W_t decreases with increased R because of lower content of matrix and thus preventing massive scale damage of matrix. Siddhartha and Gupta [37] reported that with increase in normal load, the load is distributed to overall asperities and every asperity pierces deeper into the

FIG. 7 Comparison between measured and predicted values for (a) W_t, (b) W_s, and (c) μ.

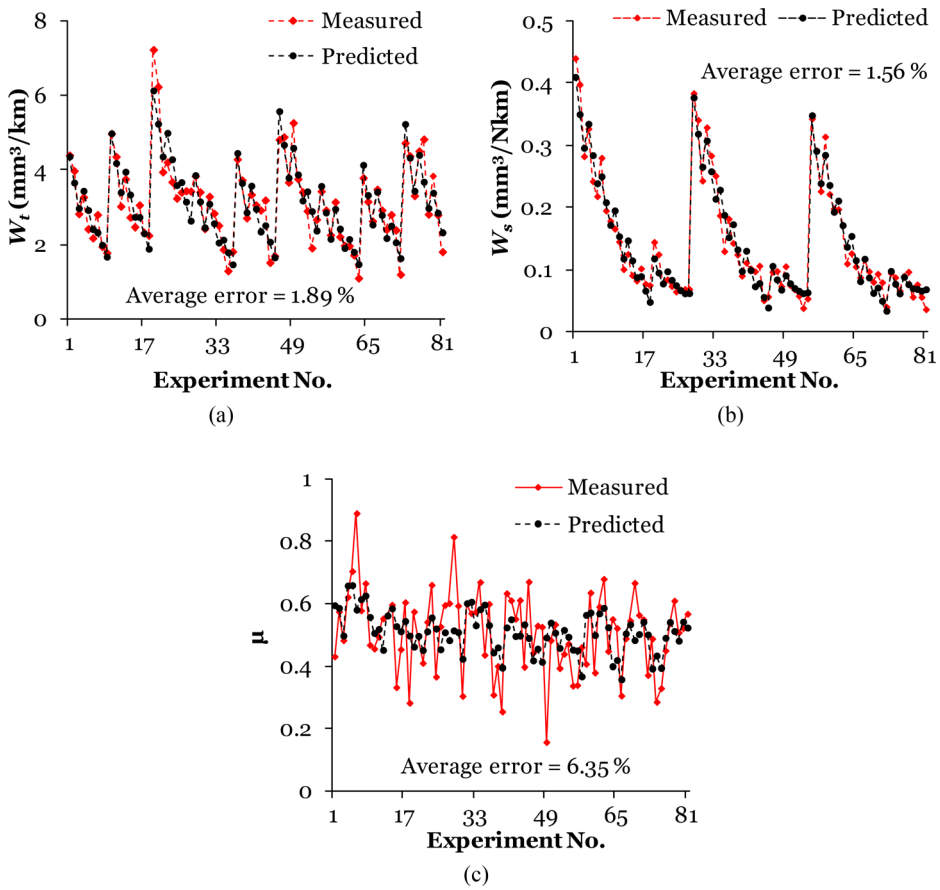

surface and thus higher W_t is obtained owing to deep grooving. **Fig. 8e** shows the W_t trend similar to **Fig. 8d**. W_t decreases with increased d and F. At higher F, wear debris assists wear mechanism in addition to frictional heating leading to localized fusion resulting in higher W_t [38]. Decline in W_t was noticed when the R is increased from 10 to 30 wt. % as seen in **Fig. 8f**.

Specific Wear Rate

Normalizing W_t with the applied load can provide further clarity in the trends. W_s with respect to v for F, d, and R is plotted in **Fig. 9a–9c**. W_s decreases with increasing v, d, and remains almost constant after 40 N. Chauhan and Thakur [33] indicated that with increased F, W_s decreases because of steadiness of transfer film on counter surface. Considerable decrease in W_s was noticed when F increased from 10 to 30 N. The effects of d and R on W_s are similar to those observed on W_t. It is observed that the combination of higher v and F is helpful for the W_s reduction. **Fig. 9d** shows that there is reduction of W_s with increase in R, which further implies that higher R is desirable for both W_t and W_s.

A comparison of **Fig. 8d** and **Fig. 9d** reveals that the load normalized W_s reduces as the F is increased. It can be observed that for 40 and 50 N loads, W_s is

FIG. 8 Model predictions for W_t with respect to v for different (a) F, (b) d, (c) R, (d) W_t with respect to R at different F. W_t with respect to d at different, (e) F, and (f) R.

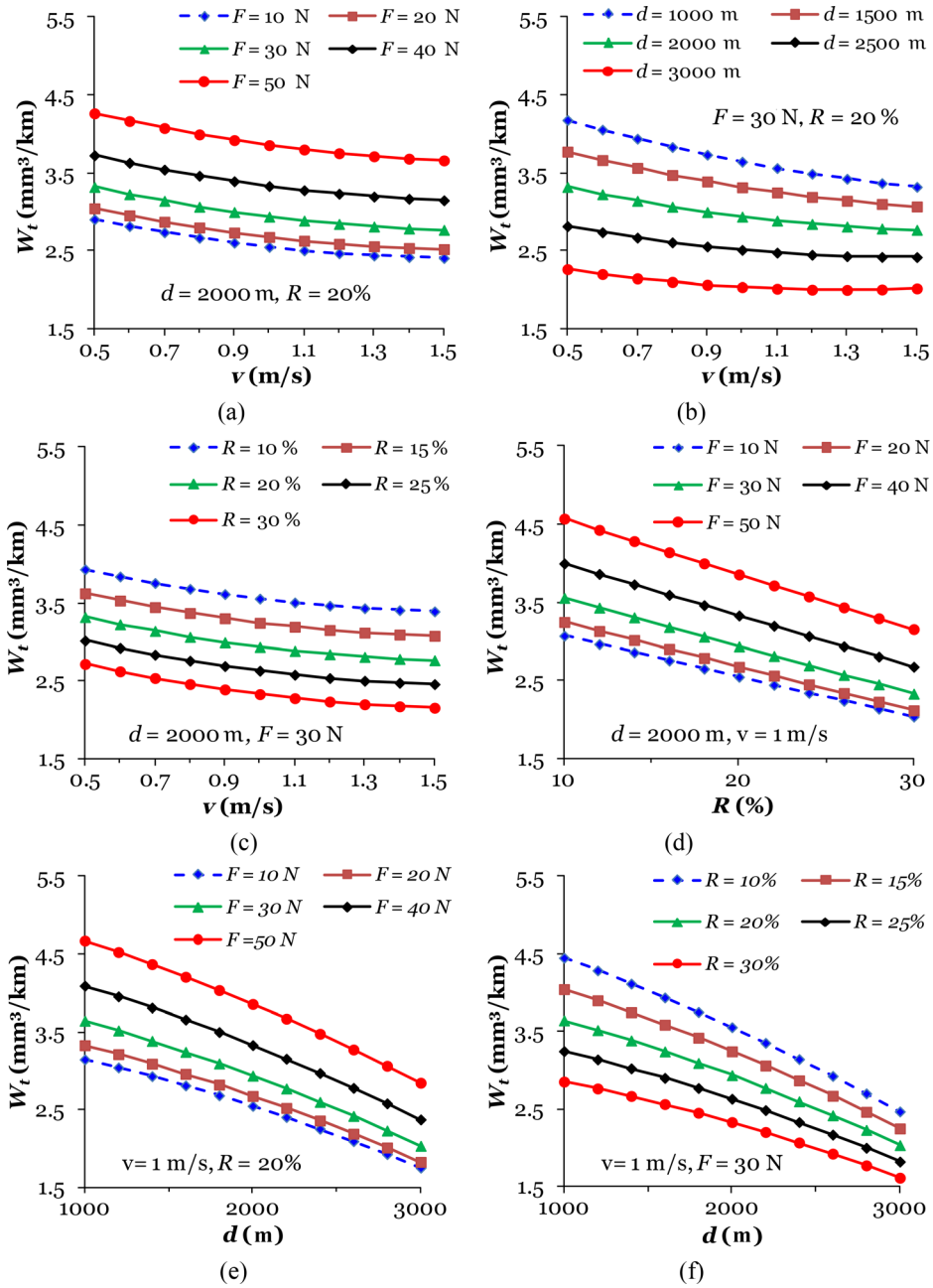

almost unchanged up to filler content of 20 wt. %. Above this value, the R is high enough to play a significant role [33,39–41]. **Fig. 9d** provides further insight that d does not have a significant influence on W_s above a critical load, which for this material seems to be 40 N. A comparison of **Fig. 9d** and **9f** reveals that a

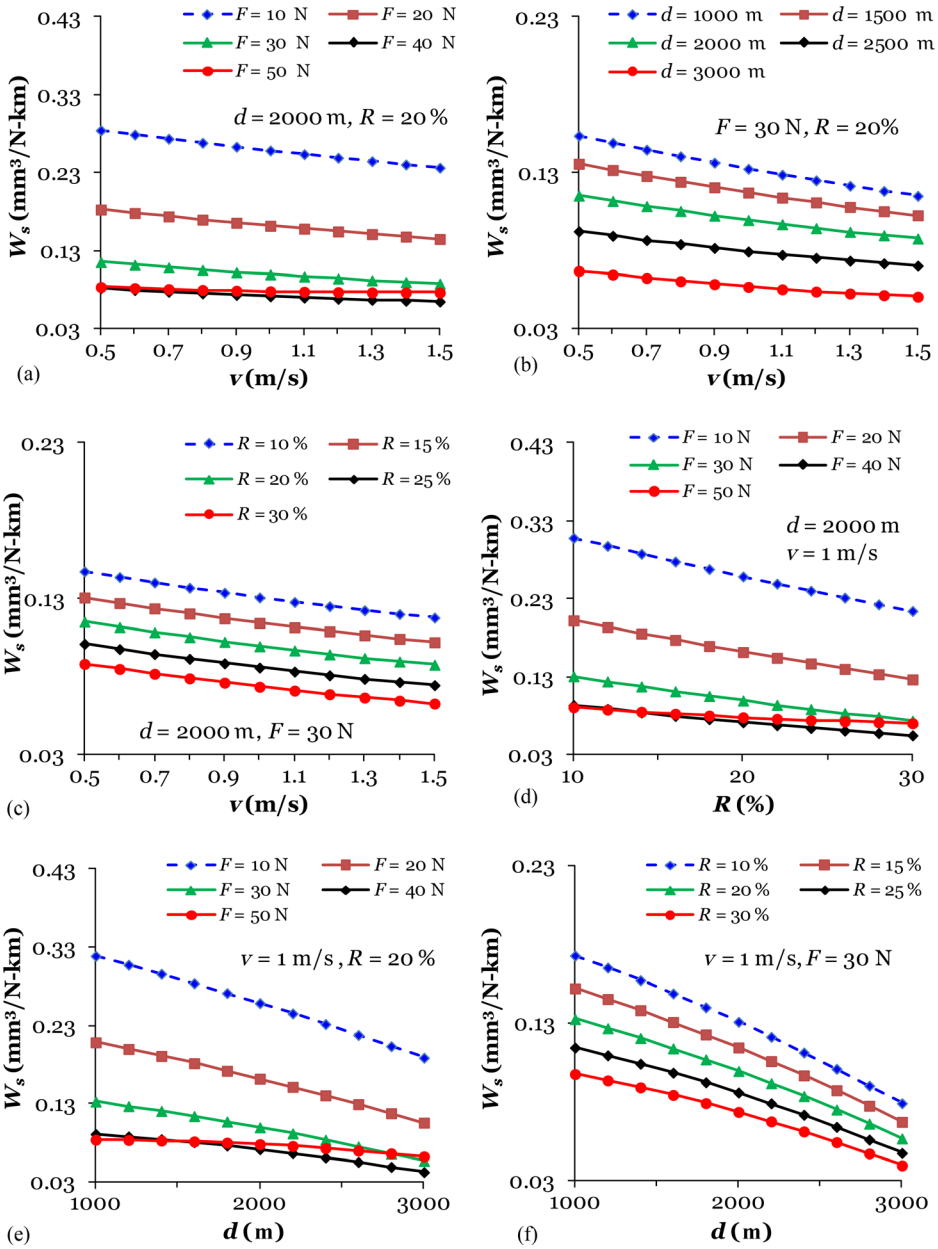

FIG. 9 Model predictions for W_s with v for different (a) F, (b) d, (c) R, (d) W_s with respect to R at different F. W_s with respect to d at different, (e) F, and (f) R.

combination of higher R and F is useful in obtaining lower W_s. W_s is drastically reduced with increasing F as seen from **Fig. 9e**. Shielding film forms because of thermal softening of the matrix at higher loads [32]. W_s increases with further increase in d as the temperature rise results in breakage of shielding film that was providing lubrication.

FIG. 10 Model predictions for μ with *v* for different (a) *F*, (b) *d*, (c) *R*, (d) μ with respect to *R* at different *F*. μ with respect to *d* at different, (e) *F*, and (f) *R*.

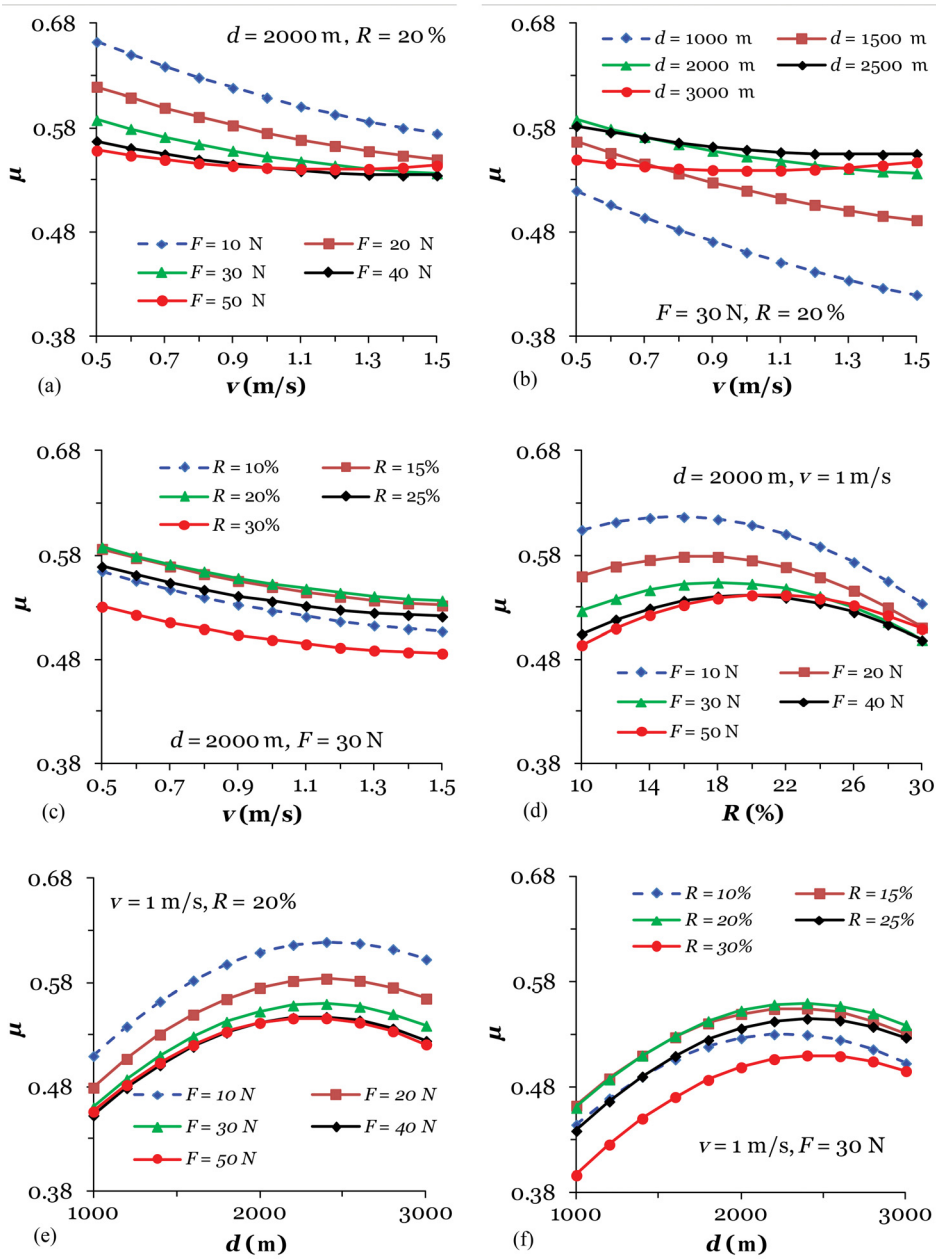

Coefficient of Friction

The variation of μ is presented in **Fig. 10**. It can be observed that the behavior of μ is non-linear and even non-monotonic with respect to some parameters such as *R* and *d*. **Fig. 10a** presents the trend of μ with *v* for specified *F*. μ decreases with increased *v* for loads in the range 10–40 N. However, for higher applied load of 50 N, μ decreases

TABLE 7

Two-way interaction parameters used in the study.

Interaction		
Parameter 1	Parameter 2	Property Investigated
v	F, d, and R	W_t
d	F, R	W_s
R	F	μ

with sliding velocity up to 1 m/s and later increases. μ decreases with increased F. Lowest μ was observed for 1.6 m/s sliding velocity with load of 40 N. Some of the constituents such as cellulose and wax may provide lubricating effect. However, the formation of the transfer film is not an intrinsic property of cellulose but is the result of complex phenomena. The transfer film is composed of fragmented walnut-shell particles, which agglomerate and adhere to the disc. On the other hand, adhesion is strongly affected by surface chemical effects: the presence of specific chemical components within the particles may promote adhesion and cohesion of walnut-shell fragments, thus facilitating the formation of the transfer film [42]. The present findings on above phenomenon of μ closely match with the experimental investigations reported in the published literature [36,43–45].

Fig. 10b depicts the divergence of μ with d. The μ decreases with v for sliding distances up to 2000 m. Lower μ was noted at 1.6 m/s sliding velocity and 1000 m sliding distance. Micro-level fluctuations might prevail in the friction coefficient with sliding distance, which is mainly attributed to the interaction of asperities between the counter surfaces during testing [35]. **Fig. 10c** exhibits the influence of filler on μ at different v. μ decreases with v for all values of R. Conversely, the μ increases with increasing R from 10 to 20 wt. % and later shows a decreasing trend. At lower R, higher volume fraction of epoxy may cause formation of a lubricating film because of its lower stiffness. Higher walnut-shell content leads to higher μ owing to presence of higher amount of deboned particles. Difference in the mechanisms of friction is likely the reason for decreasing trend of μ beyond 20 wt. % filler. The localized heat generation at higher v and subsequent matrix adhesion play a prominent role. Investigation of optimum conditions is useful for designing materials and operating conditions for the components experiencing dry sliding wear. Lowest μ was observed at sliding velocity of 1.5 m/s with R of 30 wt. %.

Irrespective of the F, μ increases with R, reaches the maximum and subsequently decreases (**Fig. 10d**). It was observed that, μ is extremely receptive to F at lower R. The minimum μ was observed at 30 wt. % and 40 N applied load. Mondal et al. [38] found that at higher load, coarser debris have greater affinity to be accumulated and compacted at craters because of the combined effect of frictional heating, material flow and applied load. It results in smoother surface and easier sliding action. **Fig. 10e** shows μ as a function of d for different F values. For any specified load, μ increases with d and decreases after reaching the peak value. Jia et al. [45] also reported the similar observation. Lower μ was observed at higher v and F. It is likely that this cycle would repeat again if the wear test is continued for longer distances. The variation in μ with filler content for different sliding distances is presented in

Fig. 10f. For given filler content, μ increases with *d* and decreases after reaching a peak at 2400 m. The minimum μ was observed at *R* of 30 wt. % for *d* of 1000 m.

Micrographic Analysis

To obtain an insight into the possible wear mechanisms during the dry sliding wear testing of walnut-shell-reinforced composites, wear surfaces of the specimens are investigated using SEM. The micrographs of representative wear-tested composites containing 10–30 wt. % walnut shells are presented in **Fig. 11**. Numerous grooves and shallow scratches can be observed in the sliding direction resembling abrasive wear [46]. At lower loads for all the filler contents, transfer film is not visible. Transfer film is prominently seen for higher filler content and loads. Presence of a higher amount of wear debris at higher values of load and filler content indicates that possible three body abrasive condition, resulting in higher wear rate.

The increase in the applied normal load causes an increase in the adhesion forces. It increases ploughing and dislodges walnut-shell particles from the surface, creating more debris (**Fig. 12a**–**12c**), which has been observed in composites previously [32]. Therefore, at higher normal load wear behavior changes from mild to severe and consequently, the depth and width of the grooves because of ploughing is increased. This increased wear rate has a direct influence on μ. The direct contact between surfaces of the specimen and disc is minimized by the presence of transfer film acting as an intermediate lubricating layer.

FIG. 11 Micrographs of the wear surfaces of representative specimens at a sliding velocity of 0.5 m/s and sliding distance of 3000 m. All micrographs are acquired at the same magnification.

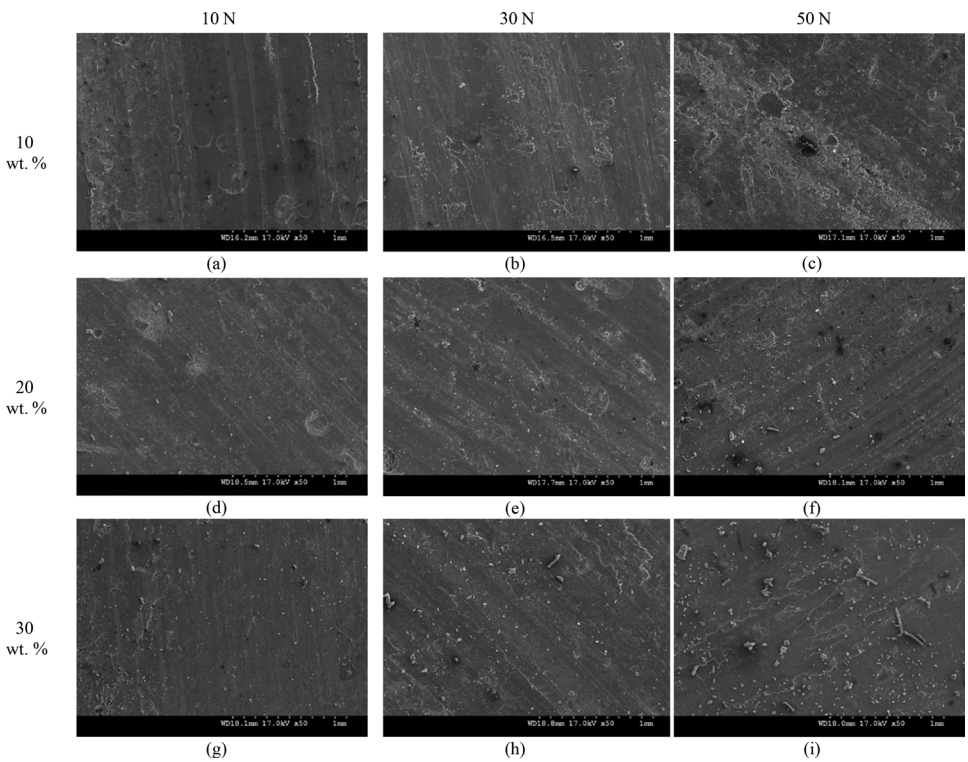

FIG. 12 Micrographs of wear surfaces of 10 wt. % walnut-shell composites at (a) 10-N, (b) 30-N, and (c) 50-N loads at sliding velocity of 0.5 m/s and sliding distance of 3000 m.

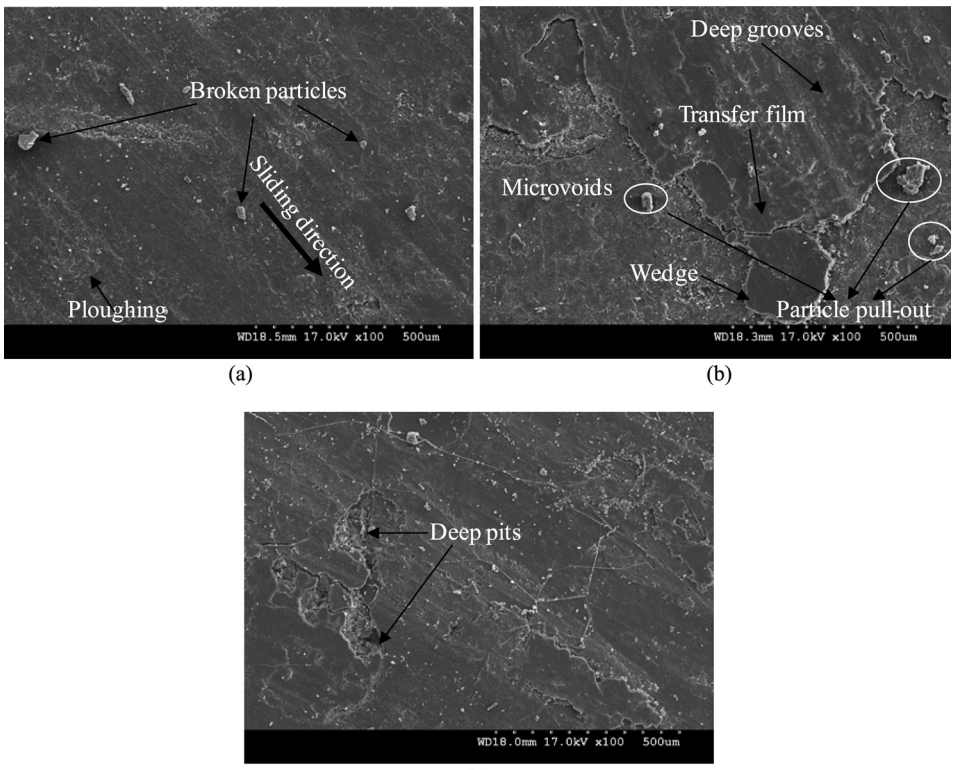

Fig. 13 shows that the dominant wear mechanism in 10 wt. % walnut shell-epoxy composite is adhesion because of presence of plastic deformation marks. Increasing the walnut-shell particle content results in higher particle debris on the contact surface. These broken particles act as third body abrasive. Adhesion and abrasion

FIG. 13 Micrographs of wear surfaces of (a) $R = 10$-wt. %, and (b) $R = 30$-wt. % walnut-shell composites at $F = 30$ N, $v = 0.5$ m/s, and $d = 3000$ m.

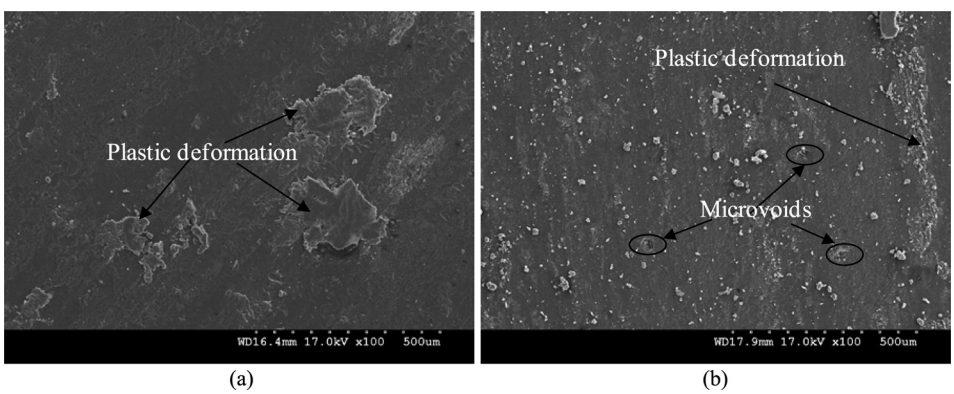

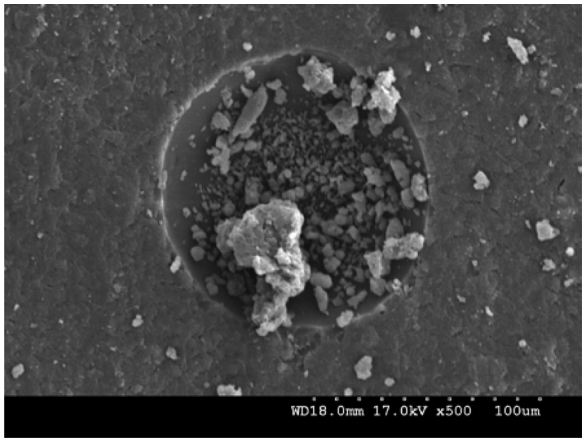

FIG. 14
Debris collected in a microvoid in the wear surface of a representative specimen at $v = 1.5$ m/s, $F = 30$ N, $d = 1000$ m, and $R = 30$ wt. %.

mechanisms are the prevailing wear mechanisms for 30 wt. % composite specimens owing to the presence of deformation marks and a large amount of wear debris. Presence of microvoids is indicated in **Fig. 13b**. **Table 2** shows that the amount of such voids is very small in the composites but their presence may play a role in wear mechanism. **Fig. 14** shows that the debris present on the wear surface may accumulate in such voids and result in lowering the wear rate. Because the void content in composites is very small in this study, this is not likely a dominant factor. However, in composites where significant porosity is present, role of voids should be investigated in greater detail.

Conclusions

Epoxy matrix composites filled with 10, 20, and 30 wt. % of walnut-shell powder were fabricated and tested for dry sliding wear test as per full factorial design (FFD) of experiments. The effects of sliding velocity, normal load, sliding distance and filler content were evaluated on wear rate, specific wear rate and coefficient of friction through RSM. Based on the experimental results and analysis the following conclusions were drawn within the selected ranges of the parameters:

- Addition of walnut shell as a filler in epoxy is effective in improving the wear resistance of composites. The composites filled with 30 wt. % walnut-shell particles showed higher W_t and lower μ than composites with lower particle content.
- W_t increases with increased F, whereas W_s and μ decrease.
- W_t and W_s decreased with increase in R, whereas μ increases.
- W_t, W_s, and μ decreased with increased v and d.
- For the range of input parameters used in this study, F is the governing parameter on the wear and friction behavior of the composites as compared to the other parameters.

Use of low-cost industrial waste fillers in developing useful composites can help in reducing the cost of composites and improving their properties as observed in this study.

ACKNOWLEDGMENTS

The writers acknowledge the support provided by BVB College of Engineering and Technology, Hubli, Karnataka, India. N.G. acknowledges support by Office of Naval Research Grant No. N00014-10-1-0988. Dear of Engineering at NYUAD is thanked for partial funding of MRD's visit to AD. The opinions of the writers expressed herein do not necessarily state or reflect those of the United States Government or the ONR, and shall not be used for advertising or product endorsement purposes. The writers thank the ME Department at NIT-K and MAE Department at NYU for providing facilities and support.

References

[1] Guo, J., Long, J., Ding, D., Wang, Q., Shan, Y., Umar, A., Zhang, X., Weeks, B. L., Wei, S., and Guo, Z., "Significantly Enhanced Mechanical and Electrical Properties of Epoxy Nanocomposites Reinforced With Low Loading of Polyaniline Nanoparticles," *RSC Adv.*, Vol. 6, No. 25, 2016, pp. 21187–21192, http://dx.doi.org/10.1039/C5RA25210E

[2] Gupta, N., Singh Brar, B., and Woldesenbet, E., "Effect of Filler Addition on the Compressive and Impact Properties of Glass Fibre Reinforced Epoxy," *Bull. Mater. Sci.*, Vol. 24, No. 2, 2001, pp. 219–223, http://dx.doi.org/10.1007/BF02710105

[3] Gupta, N., Lin, T. C., and Shapiro, M., "Clay-Epoxy Nanocomposites: Processing and Properties," *JOM*, Vol. 59, No. 3, 2007, pp. 61–65, http://dx.doi.org/10.1007/s11837-007-0041-4

[4] Patnaik, A., Satapathy, A., Dwivedy, M., and Biswas, S., "Wear Behavior of Plant Fiber (Pine-Bark) and Cement Kiln Dust-Reinforced Polyester Composites Using Taguchi Experimental Model," *J. Compos. Mater.*, Vol. 44, No. 5, 2010, pp. 559–574, http://dx.doi.org/10.1177/0021998309346547

[5] Bolton, J., "The Potential of Plant Fibers as Crops for Industrial Use," *Outlook Agric.*, Vol. 24, No. 2, 1995, pp. 85–89.

[6] Risby, M. S., Wong, S. V., Hamouda, A. M. S., Khairul, A. R., and Elsadig, M., "Ballistic Performance of Coconut Shell Powder/Twaron Fabric Against Non-Armour Piercing Projectiles," *Def. Sci. J.*, Vol. 58, No. 2, 2008, pp. 248–263, http://dx.doi.org/10.14429/dsj.58.1645

[7] Bledzki, A. K. and Gassan, J., "Composites Reinforced With Cellulose Based Fibres," *Prog. Polym. Sci.*, Vol. 24, No. 2, 1999, pp. 221–274, http://dx.doi.org/10.1016/S0079-6700(98)00018-5

[8] Pirayesh, H., Khazaeian, A., and Tabarsa, T., "The Potential for Using Walnut (*Juglans Regia* L.) Shell as a Raw Material for Wood-Based Particleboard Manufacturing," *Compos. Part B: Eng.*, Vol. 43, No. 8, 2012, pp. 3276–3280, http://dx.doi.org/10.1016/j.compositesb.2012.02.016

[9] Kulkarni, M. C., "Characterization of Light Weight Composite Proppants," M.S. thesis, Texas A&M University, College Station, TX, 2008.

[10] Demirbaş, A., "Estimating of Structural Composition of Wood and Non-Wood Biomass Samples," *Energy Sources*, Vol. 27, No. 8, 2005, pp. 761–767, http://dx.doi.org/10.1080/00908310490450971

[11] Chen, Y. and Cheng, X., "Research on Characteristic of Walnut Shell High Boiling Solvent Lignin by Chemical Analysis, IR and NMR," *International*

Conference on Remote Sensing, Environment and Transportation Engineering (RSETE), Nanjing, China, 24–26 June 2011.

[12] Friedrich, K., Lu, Z., and Häger, A. M., "Overview on Polymer Composites for Friction and Wear Application," *Theor. Appl. Fract. Mech.*, Vol. 19, No. 1, 1993, pp. 1–11, http://dx.doi.org/10.1016/0167-8442(93)90029-B

[13] Kishore, A. and Sridhar, G. B., "On Evaluating Erosion by Sand Particles in Polythene System Without and With Ceramic Particles," *Polym. Test.*, Vol. 21, No. 4, 2002, pp. 473–477, http://dx.doi.org/10.1016/S0142-9418(01)00112-X

[14] Singh, A. K. and Siddhartha, "Leverage of Cenosphere Filler Size on Mechanical and Dry Sliding Wear Peculiarity of Polyester Composites," *J. Compos. Mater.*, Vol. 49, No. 22, 2015, pp. 2789–2802, http://dx.doi.org/10.1177/0021998314554436

[15] Thakur, S. and Chauhan, S., "Friction and Sliding Wear Characteristics Study of Submicron Size Cenosphere Particles Filled Vinylester Composites Using Taguchi Design of Experimental Technique," *J. Compos. Mater.*, Vol. 48, No. 23, 2014, pp. 2831–2842, http://dx.doi.org/10.1177/0021998313502740

[16] Souza, J. R., Silva, R. C., Silva, L. V., Medeiros, J. T., Amico, S. C., and Brostow, W., "Tribology of Composites Produced With Recycled GFRP Waste," *J. Compos. Mater.*, Vol. 49, No. 23, 2015, pp. 2849–2858, http://dx.doi.org/10.1177/0021998314557296

[17] Arivalagan, P., Suresha, B., Chandramohan, G., Krishnaraj, V., and Palaniappan, N., "Mechanical and Abrasive Wear Behavior of Carbon Fabric Reinforced Epoxy Composite With and Without Fly Ash Cenospheres," *J. Compos. Mater.*, Vol. 47, No. 23, 2013, pp. 2925–2935, http://dx.doi.org/10.1177/0021998312459872

[18] Bahadur, S. and Sunkara, C., "Effect of Transfer Film Structure, Composition and Bonding on the Tribological Behavior of Polyphenylene Sulfide Filled With Nano Particles of TiO2, ZnO, CuO and SiC," *Wear*, Vol. 258, No. 9, 2005, pp. 1411–1421, http://dx.doi.org/10.1016/j.wear.2004.08.009

[19] Wetzel, B., Haupert, F., Friedrich, K., Zhang, M. Q., and Rong, M. Z., "Impact and Wear Resistance of Polymer Nanocomposites at Low Filler Content," *Polym. Eng. Sci.*, Vol. 42, No. 9, 2002, pp. 1919–1927, http://dx.doi.org/10.1002/pen.11084

[20] Nitin, S. and Singh, V. K., "Mechanical Behaviour of Walnut Reinforced Composite," *J. Mater. Environ. Sci.*, Vol. 4, No. 2, 2013, pp. 233–238.

[21] Zahedi, M., Pirayesh, H., Khanjanzadeh, H., and Tabar, M. M., "Organo-Modified Montmorillonite Reinforced Walnut Shell/Polypropylene Composites," *Mater. Des.*, Vol. 51, 2013, pp. 803–809, http://dx.doi.org/10.1016/j.matdes.2013.05.007

[22] Srivastava, N., Singh, V. K., and Bhaskar, J., "Compressive Behavior of Walnut (*Juglans* L.) Shell Particles Reinforced Composite," *Usak Univ. J. Mater. Sci.*, Vol. 1, 2013, pp. 23–30.

[23] Ayrilmis, N., Kaymakci, A., and Ozdemir, F., "Physical, Mechanical, and Thermal Properties of Polypropylene Composites Filled With Walnut Shell Flour," *J. Ind. Eng. Chem.*, Vol. 19, No. 3, 2013, pp. 908–914, http://dx.doi.org/10.1016/j.jiec.2012.11.006

[24] Qi, S., Fu, Z., Yun, R., Jiang, S., Zheng, X., Lu, Y., Matejka, V., Kukutschova, J., Peknikova, V., and Prikasky, M., "Effects of Walnut Shells on Friction and

Wear Performance of Eco-Friendly Brake Friction Composites," *Proc. Inst. Mech. Eng., Part J: J. Eng. Tribol.*, Vol. 228, No. 5, 2014, pp. 511–520, http://dx.doi.org/10.1177/1350650113517112

[25] Mohammed, A. J., "Study the Effect of Adding Powder Walnut Shells on the Mechanical Properties and the Flame Resistance for Low Density Polyethylene (LDPE)," *Int. J. Sci. Technol.*, Vol. 3, No. 1, 2014, pp. 18–22.

[26] Myers, R. H., Montgomery, D. C., and Anderson-Cook, C. M., *Response Surface Methodology: Process and Product Optimization Using Designed Experiments*, Wiley, Hoboken, NJ, 2009.

[27] Montgomery, D. C., *Design and Analysis of Experiments*, Wiley, Hoboken, NJ, 2003.

[28] Manakari, V., Parande, G., Doddamani, M., Gaitonde, V. N., Siddhalingeshwar, I. G., Kishore, Shunmugasamy, V. C., and Gupta, N., "Dry Sliding Wear of Epoxy/Cenosphere Syntactic Foams," *Tribol. Int.*, Vol. 92, 2015, pp. 425–438.

[29] ASTM G99-05, A. *Standard Test Method for Wear Testing with a Pin-on-Disc Apparatus.* 2010, ASTM International, West Conshohocken, PA, 2007, www.astm.org

[30] Ravikiran, A. and Surappa, M. K., "Oscillations in Coefficient of Friction During Dry Sliding of A356 Al-30 % WT *SiCp* MMC Against Steel," *Scripta Mater.*, Vol. 36, No. 1, 1997, pp. 95–98.

[31] Montgomery, D. C., *Design and Analysis of Experiments*, Wiley, Hoboken, NJ, 2006.

[32] Chauhan, S. R. and Thakur, S., "Effects of Particle Size, Particle Loading and Sliding Distance on the Friction and Wear Properties of Cenosphere Particulate Filled Vinylester Composites," *Mater. Des.*, Vol. 51, 2013, pp. 398–408.

[33] Chauhan, S. and Thakur, S., "Effect of Micro Size Cenosphere Particles Reinforcement on Tribological Characteristics of Vinylester Composites Under Dry Sliding Conditions," *J. Miner. Mater. Character. Eng.*, Vol. 11, No. 10, 2012, pp. 938–946.

[34] Kanchanomai, C., Noraphaiphipaksa, N., and Mutoh, Y., "Wear Characteristic of Epoxy Resin Filled With Crushed-Silica Particles," *Compos. Part B: Eng.*, Vol. 42, No. 6, 2011, pp. 1446–1452.

[35] Rao, R. N. and Das, S., "Effect of Sliding Distance on the Wear and Friction Behavior of as Cast and Heat-Treated Al–SiCp Composites," *Mater. Des.*, Vol. 32, No. 5, 2011, pp. 3051–3058.

[36] Xing, X. S. and Li, R. K. Y., "Wear Behavior of Epoxy Matrix Composites Filled With Uniform Sized Sub-Micron Spherical Silica Particles," *Wear*, Vol. 256, Nos. 1–2, 2004, pp. 21–26.

[37] Siddhartha and Gupta, K., "Mechanical and Abrasive Wear Characterization of Bidirectional and Chopped E-Glass Fiber Reinforced Composite Materials," *Mater. Des.*, Vol. 35, 2012, pp. 467–479.

[38] Mondal, D. P., Das, S., and Jha, N., "Dry Sliding Wear Behaviour of Aluminum Syntactic Foam," *Mater. Des.*, Vol. 30, No. 7, 2009, pp. 2563–2568.

[39] Zhang, M. Q., Rong, M. Z., Yu, S. L., Wetzel, B., and Friedrich, K., "Effect of Particle Surface Treatment on the Tribological Performance of Epoxy Based Nanocomposites," *Wear*, Vol. 253, Nos. 9–10, 2002, pp. 1086–1093.

[40] Jawahar, P., Gnanamoorthy, R., and Balasubramanian, M., "Tribological Behaviour of Clay–Thermoset Polyester Nanocomposites," *Wear*, Vol. 261, Nos. 7–8, 2006, pp. 835–840.

[41] Friedrich, K., Zhang, Z., and Schlarb, A. K., "Effects of Various Fillers on the Sliding Wear of Polymer Composites," *Compos. Sci. Technol.*, Vol. 65, Nos. 15–16, 2005, pp. 2329–2343.

[42] Chand, N. and Fahim, M., *Tribology of Natural Fiber Polymer Composites*, 1st ed., Woodhead, Cambridge, UK, 2008, 220 pp.

[43] Chang, L. and Friedrich, K., "Enhancement Effect of Nanoparticles on the Sliding Wear of Short Fiber-Reinforced Polymer Composites: A Critical Discussion of Wear Mechanisms," *Tribol. Int.*, Vol. 43, No. 12, 2010, pp. 2355–2364.

[44] Dharmalingam, S., Subramanian, R., and Somasundara Vinoth, K., "Analysis of Dry Sliding Friction and Wear Behavior of Aluminum-Alumina Composites Using Taguchi's Techniques," *J. Compos. Mater.*, Vol. 44, No. 18, 2010, pp. 2161–2177.

[45] Jia, B.-B., Li, T.-S., Liu, X.-J., and Cong, P.-H., "Tribological Behaviors of Several Polymer–Polymer Sliding Combinations Under Dry Friction and Oil-Lubricated Conditions," *Wear*, Vol. 262, Nos. 11–12, 2007, pp. 1353–1359.

[46] Tabandeh-Khorshid, M., Omrani, E., Menezes, P. L., and Rohatgi, P. K., "Tribological Performance of Self-Lubricating Aluminum Matrix Nanocomposites: Role of Graphene Nanoplatelets," *Eng. Sci. Technol.*, Vol. 19, No. 1, 2016, pp. 463–469.